ORIGINAL RESEARCH

In vitro and in vivo targeting imaging of pancreatic cancer using a $Fe_3O_4@SiO_2$ nanoprobe modified with anti-mesothelin antibody

Fang Liu[1,*]
Wenjun Le[2,*]
Tianxiao Mei[2]
Tiegong Wang[1]
Luguang Chen[1]
Yi Lei[1]
Shaobin Cui[2]
Bingdi Chen[2]
Zheng Cui[2,3]
Chengwei Shao[1]

[1]Radiology Department of Changhai Hospital, Second Military Medical University, [2]Shanghai East Hospital, The Institute for Biomedical Engineering & Nano Science, Tongji University School of Medicine, Shanghai, People's Republic of China; [3]Department of Pathology, Wake Forest University School of Medicine, Winston-Salem, NC, USA

*These authors contributed equally to this work

Correspondence: Bingdi Chen
Shanghai East Hospital, The Institute for Biomedical Engineering & Nano Science, Tongji University School of Medicine, No 1239 Siping Road, Shanghai 200120, People's Republic of China
Tel +86 21 6598 3706
Fax +86 21 6598 3706
Email inanochen@tongji.edu.cn

Chengwei Shao
Radiology Department of Changhai Hospital, Second Military Medical University 168 Changhai Rd, Shanghai 200433, People's Republic of China
Tel +86 21 3116 2148
Fax +86 21 3116 2148
Email cwshao@sina.com

Abstract: Pancreatic cancer is a highly malignant disease with a 5-year survival rate $<5\%$ mainly due to lack of early diagnosis and effective therapy. In an effort to improve the early diagnostic rate of pancreatic cancer, a nanoprobe $Fe_3O_4@SiO_2$ modified with anti-mesothelin antibody (A-MFS) was prepared to target cells and tumor tissues highly expressing mesothelin in vitro (human pancreatic cancer cell line SW1990) and in vivo (subcutaneously transplanted tumors) studies. The A-MFS probe was successfully prepared and was spherical and uniform with a hydrodynamic diameter between 110 and 130 nm. Cell Counting Kit-8 testing indicated that A-MFS was nontoxic in vitro and in vivo studies. The in vitro study showed that the A-MFS probe specifically targeted SW1990 cells with high mesothelin expression. The in vivo study was conducted in Siemens 3.0 T magnetic resonance imaging. The average T2-weighted signal values of the xenografts were 966.533 ± 31.56 before injecting A-MFS and 691.133 ± 56.84 before injecting saline solution. After injection of 0.1 mL A-MFS via nude mouse caudal vein for 2.5 hours, the average T2-weighted signal of the xenograft decreased by 342.533 ± 42.6. The signal value decreased by -61.233 ± 33.9 and -58.7 ± 19.4 after injection of the saline and $Fe_3O_4@SiO_2$. The decrease of tumor signal by A-MFS was much more significant than that by saline and $Fe_3O_4@SiO_2$ ($P<0.05$). The results demonstrated the high stability and nontoxicity of A-MFS, which effectively targeted pancreatic cancer in vitro and in vivo. A-MFS is a promising agent for diagnosis of pancreatic cancer.

Keywords: nanoprobe, mesothelin, $Fe_3O_4@SiO_2$, pancreatic cancer, targeted imaging

Introduction

Pancreatic cancer is one of the most highly malignant tumors with similar rates of incidence and mortality. Research advances over the past few decades failed to improve the survival rate. The overall 5-year survival rate still remains $<5\%$ since most patients newly diagnosed with pancreatic cancer have already advanced in the disease and are not amenable to surgical therapy.[1–4] Early and definitive diagnosis and prompt therapy significantly improve the prognosis and increase survival rates.[5] Molecular imaging is a potential way to improve early diagnosis.

Molecular imaging of biological processes in vivo enables the detection of molecular and cellular mutations and the pathological changes at an early stage of the disease and promotes early diagnosis and treatment.[6–8] CA19-9 is a clinical biomarker widely used, but lacks specificity and sensitivity for early diagnosis of pancreatic cancer.[9,10] Therefore, discovery of highly-specific tumor biomarkers is imperative. Nanomedicine involves application of nanoscience and technology to medicine. Targeted labeling entails combining nanosized materials with biomarkers to synthesize multifunctional

complexes and target functional biomarkers to specific cells or tissues in vitro and in vivo.

In recent decades, several serum and tissue biomarkers in pancreatic cancer have demonstrated the benefit of early diagnosis. The high-molecular weight mucins are a family of extracellular proteins that are heavily glycosylated with complex oligosaccharides and play an important role in tumor formation and progression.[11] Mucins 1 and 4 are associated with pancreatic cancer.[12,13] A study[14] suggest that BxPC-3 and Panc-1 cell lines of pancreatic cancer express mucin 1. They also demonstrated that subcutaneous and orthotopic tumor transplantation emits strong fluorescence signals after injection of fluorophore-conjugated anti-MUC1 antibodies via nude mice tail veins. Wu et al[15] prepared new multifunctional nanoparticles (MnMEIO-silane-NH$_2$-[MUC4]-mPEG nanoparticles) containing MUC4 antibodies as a new type of magnetic resonance imaging (MRI) and optical imaging contrast agent. The new type of contrast agent selectively and specifically targeted mucin-expressing tumor tissues in nude mice. Survivin gene, which is a member of the inhibitor of apoptosis family, is abundantly expressed in the serum of most pancreatic cancer patients.[16,17] Tong et al[18] synthesized a survivin gene-targeted magnetic iron oxide nanoparticle with high stability and without any toxicity. The magnetic molecular probe selectively targeted the pancreatic cancer cells with survivin gene expression. Urokinase plasminogen activator receptor, a cellular receptor, is expressed in >86% of pancreatic cancer tissues, but not in normal or chronic pancreatitis tissues. It also contributes to tumor progression.[19,20] Studies have shown that urokinase plasminogen activator receptor-targeted nanoparticles selectively accumulate in transplanted tumor lesions of human pancreatic cancer in nude mice.[21] Despite advances involving new biomarkers for pancreatic cancer, none of them has been validated for routine clinical use. Therefore, additional studies have been undertaken to develop or discover specific markers targeting pancreatic cancer and generate novel nanoparticles for clinical use.

Mesothelin (MSLN), which is overexpressed in several tumors, such as mesothelioma, ovarian cancer, and pancreatic cancer, is a 40 kDa cell surface glycoprotein. It is selectively expressed in malignant pancreatic cancer tissue, but not in pancreatic benign tumors, acute or chronic pancreatitis, and normal pancreatic tissues.[22,23] MSLN plays an important role in the development of pancreatic cancer in different ways. The overexpression of MSLN promotes the motility, increases the proliferation, and inhibits the apoptosis of pancreatic cancer cells, and is associated with tumor invasion

and migration. Strong expression of MSLN usually indicates poor prognosis.[24–27] It is considered as a potential and promising diagnostic, imaging, and therapeutic biomarker in pancreatic cancer.[28]

Fe$_3$O$_4$ nanoparticles are the most common superparamagnetic iron oxide components used as multifunctional nanoparticles. Their unique superparamagnetic properties, biocompatibility, and ease of preparation have wide biomedical applications.[29,30] Silica is a good surface modifier because of its nontoxicity, high stability, water dispersibility, and excellent biocompatibility.[31] It easily facilitates conjugation with various functional groups and enables the coupling and labeling of biological targets with selectivity and specificity.[32] Superparamagnetic iron oxide nanoparticles (SPIONs) covered with silica shells (Fe$_3$O$_4$@SiO$_2$ [FS]) are potentially the most effective carriers for delivering specific markers and drugs to target sites in the human body.[33] In this study, we synthesized multifunctional nanoprobe FS modified with MSLN antibody. Our team investigated its labeling ability in pancreatic cancer in vitro and in vivo for possible clinical application as a novel molecular probe.

Materials and methods
Materials
All initial reagents were obtained commercially and used as-received: sodium acetate, iron trichloride hexahydrate (FeCl$_3$·6H$_2$O), ethylene glycol, ethanol, deionization water (DI water), ammonium hydroxide, tetraethylorthosilicate, (3-aminopropyl)triethoxysilane, polyethylene glycol (PEG) diacid solution (molecular weight, 6,000), 1-ethyl-3-(3-dimethylaminopropyl)carbodiimide hydrochloride (EDC·HCl), borate saline buffer (50 mM, pH 8.2), phosphate-buffered saline (PBS), bovine serum albumin, sodium azide, microplate reader, Cell Counting Kit-8 (CCK-8), formazan dye, dehydrogenase, pancreatin, and mesothelin antibody (R&D Systems, Inc., Minneapolis, MN, USA).

Cell lines
Human pancreatic cancer SW1990 cell line was supplied by the Department of Gastroenterology, the first hospital affiliated to the Second Military Medical University in Shanghai, People's Republic of China. The research is approved and performed under the ethical and legal standards of Ethics Committee of Second Military Medical University. The cells were maintained in Roswell Park Memorial Institute (RPMI) 1640 medium supplemented with 10% fetal bovine serum, penicillin–streptomycin solution (100×), and were

cultured at 37°C in a humidified atmosphere containing 5% CO_2 incubator.

Nude mice
Male, 4- to 6-week-old athymic nude mice (BALB/C), weighing 18±2 g, were purchased from the Laboratory Animal Center of the Second Military Medical University, Shanghai, People's Republic of China, and raised under specific pathogen-free conditions at a constant temperature of 25°C–27°C and humidity of 40%–50%. The animal experiments were approved and performed in accordance with the guidelines of the Animal Protection and Care Committee of the Second Military Medical University. The number of animal ethics is 13071002132.

Preparation of pancreas cancer xenografts
The density of logarithmic phase SW1990 cell suspension was adjusted to 2×10^7/mL with PBS. An amount of 0.1 mL of the cell suspension was injected subcutaneously, respectively, into the right axillas of nude mice. These mice continued to be raised under specific pathogen-free conditions in the Laboratory Animal Center.

Preparation of nanoprobe Fe_3O_4 (nanoparticles)
The magnetic microspheres were prepared by a solvothermal reaction.[34] Using 2.56 g of sodium acetate and 0.86 g of $FeCl_3 \cdot 6H_2O$ dissolved in 30 mL of ethylene glycol under vigorous magnetic stirring. The homogeneous yellow solution was transferred to Teflon-lined stainless-steel autoclave and heated at 200°C for nearly 8 hours, and cooled to room temperature. Each of the products was washed three times with ethanol and DI water and redispersed into DI water for use.

Preparation of the FS-NH_2 probe
An aqueous dispersion of 5 mL of Fe_3O_4 (50 mg/mL) was treated with 0.1 M HCl aqueous solution under sonication for 15 minutes. The treated Fe_3O_4 microspheres were dispersed in a mixture of ethanol and water (v/v=70/30) briefly. The pH was adjusted to ~9.5 by addition of ammonium hydroxide. Later, 80 µL of tetraethylorthosilicate was poured into the reactor with vigorous stirring at room temperature for ~24 hours. To graft amino groups,[35] 50 mL (3-aminopropyl)triethoxysilane was injected into the system under stirring for 4 hours. Methanol was then added to precipitate the product. Following centrifugation, the product

was washed with ethanol several times, and finally dispersed in deionized water.

Synthesis of FS probe modified with anti-MSLN antibody
The amino-silane-coated magnetite particles were mixed with PEG diacid solution (molecular weight, 6,000) in the ratio of 1:2, followed by the addition of 5 mg of EDC·HCl to the solution. The solution was stirred overnight at room temperature. The resulting product (FS/PEG) was purified by ethanol and DI water, each three times, and redispersed into borate saline buffer (50 mM, pH 8.2) for conjugation with anti-MSLN antibody using EDC·HCl as the cross-linker. The FS/PEG was reacted with nanoparticles:anti-MSLN antibody:EDC·HCl in the molar ratio of 1:10:4,000 in a borate saline buffer (50 mM, pH 8.2) under continuous stirring for 2 hours at room temperature. The final bioconjugates were dispersed in PBS (0.01 M, pH 7.4, 0.5% bovine serum albumin, 0.02% sodium azide) after magnetic separation and washed with 0.01 M PBS (pH 7.4) twice.

Characterization of A-MFS
The morphology of the material was observed by transmission electron microscopy using a JEM-2100F electron microscope (JEOL Ltd., Tokyo, Japan), and its hydrodynamic diameter was measured by nanoparticle size analyzer (NanoZS90). The stability test of A-MFS can be found in the Supplementary Materials. The longitudinal (T1) and transverse (T2) relaxation times of A-MFS were measured with a 1.41 T minispec mq 60 NMR Analyzer (Bruker, Karlsruhe, Germany) at 37°C. Relaxivity values of r1 and r2 were calculated by fitting the 1/T1 and 1/T2 relaxation time (s^{-1}) versus Fe concentration (mM) curves. X-ray photoelectron spectroscopy was used to detect chemical elements of A-MFS.

Cell toxicity
The cytotoxicity of the nanoprobe FS modified with anti-MSLN antibody against human pancreatic cancer SW1990 cells was determined by measuring the inhibition of the cell growth using a CCK-8 assay. SW1990 cells were first seeded in a 96-well plate at a density of 5,000 cells/well and incubated overnight at 37°C and 5% CO_2 in an incubator. Next, three wells of SW1990 cells were incubated with various concentrations of magnetic vesicles (0, 100, 200, 300, 400, and 500 mg/L) for 2, 6, and 24 hours, respectively. Each well was then supplemented with 10 µL CCK solution, followed by incubation of the culture plate for 1 to 4 hours. Eventually, the absorbance at 450 nm was measured using a microplate reader

to determine the number of live cells indirectly. The cell viability was measured by calculating the amount of formazan dye generated by the activity of cellular dehydrogenases, which was directly proportional to the number of living cells.

In vitro targeting

Pancreatic cancer cell line SW1990 supplied by the Department of Digestive Diseases of Changhai Hospital (Shanghai, People's Republic of China) was cultured. In order to test the targeting ability of the A-MFS with SW1990 cells in vitro, red fluorescence quantum dots, which are water-soluble, were added to both the probes FS and A-MFS to synthesize fluorescence nanomaterials. The SW1990 cells in the logarithmic phase were incubated with 5 µL of fluorescent nanoprobes (1 mg/mL) FS and A-MFS, respectively, for 30 minutes. LM-3, a human liver cancer cell line, was provided by The Institute for Biomedical Engineering and Nano Science at Tongji University School of Medicine, Shanghai, People's Republic of China. LM-3 cells in the logarithmic phase were also incubated with 5 µL of fluorescent nanoprobe A-MFS (1 mg/mL) for 30 minutes. After incubation, cells in the three groups were visualized through fluorescence microscope to determine the different effects of FS and A-MFS on SW1990 and LM-3 cells.

The SW1990 and LM-3 cells were digested with pancreatin, and the supernatant was discarded after centrifugation. The sample was analyzed by flow cytometry, after cells were washed with 300 µL PBS.

In vivo MRI

In this study, all the mice were successfully developed into subcutaneously transplanted tumor models. When the diameter of subcutaneously transplanted tumor reached 1.0 cm, nine mice were divided into three groups randomly. The control group of mice received an intravenous injection of 0.1 mL saline solution via caudal veins. The other two groups were injected with 1 mg/mL of FS and A-MFS solution (0.1 mL per mouse), respectively, via caudal veins. All the images of mice were obtained using Siemens 3.0 T magnetic resonance scanner. Before MRI imaging, 1% pentobarbital sodium (75 mL/kg) was injected into the abdominal cavity to ensure that the mice were anesthetized. Mouse limbs were fixed by adhesive tape on hardboard and replaced into the finger coil. Images were obtained before and after 30 minutes, 1, 2, 2.5, and 3 hours following intravenous injection of the solution, respectively. The MRI scan range exceeded the tumor size. T2WI axial and coronal images of fast spin echo were captured at each phase. Specific imaging parameters were as follows: T2-weighted fast echo-spin axial of field

of view =60×48.8 mm, slice thickness =2 mm, repetition time =3,500 ms, echo time =92 ms, resolution ratio =192×192, voxel size =0.3×0.3×2.0 mm; the T2-weighted fast echo-spin coronal of field of view =80×65 mm, slice thickness =2 mm, repetition time =3,500 ms, echo time =92 ms, resolution ratio =192×192, and voxel size =0.4×0.4×2.0 mm. We selected the regions of interest measuring 2 mm^2 on the tumor solid component of each phase to measure signal values, after all the images were captured.

Test of Fe distribution in vivo

The organs and tissues, including liver, spleen, kidney, heart, lung, and tumor were collected from the anesthetized mice ~2.5 hours after injection with FS or A-MFS. They were eroded with concentrated nitric acid to determine the biodistribution of Fe using inductively coupled plasma-atomic emission spectrometry.

Histochemistry

Following MR scanning, two mice from control and experimental groups were killed by cervical dislocation at an appropriate time. Heart, liver, spleen, lung, and kidney were removed to obtain routine paraffin sections. These tissues were embedded in 10% buffered formaldehyde, followed by paraffin for hematoxylin and eosin staining to observe the pathological changes in the organs of the two groups. An experienced pathologist with >5 years of experience reviewed the microscopic images of the tissues.

Transmission electron microscopy

Mice in the experimental group injected with A-MFS were dissected after in vivo MRI. Tumor tissue was then cut into ultrathin sections and observed under a transmission electron microscope.

Statistical analysis

The signal values were recorded as mean ± standard. Student's unpaired t-test was used to analyze the differences between experimental and control groups. A P-value below 0.05 was considered statistically significant.
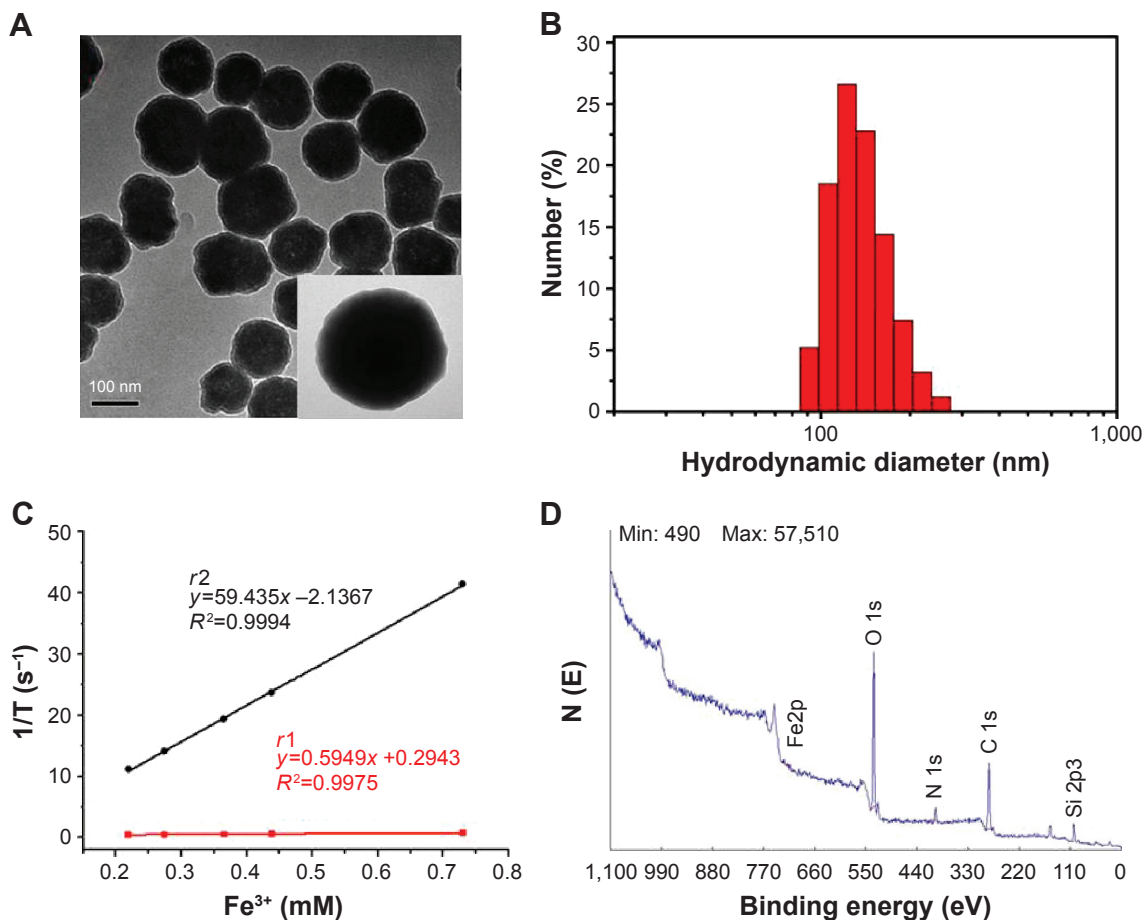
Results
Characterization of the nanoprobe

The procedure outlining construction of FS modified with anti-MSLN antibodies is shown in Figure 1. The morphological structure of the probe, the distribution of hydrodynamic diameters relaxation rate, and X-ray photoelectron spectroscopy results are shown in Figure 2. The probe FS modified with anti-MSLN antibodies is spherical and regular in shape.
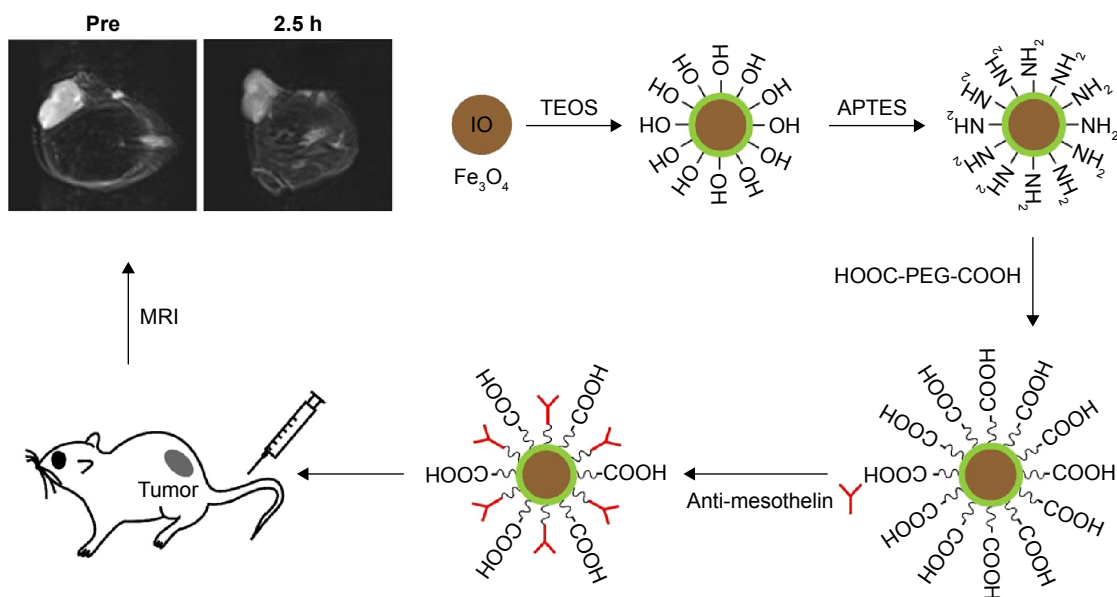
Figure 1 Schematic diagram illustrating the preparation of A-MFS probe and its T2-weighted images.
Abbreviations: IO, Fe_3O_4; A-MFS, $Fe_3O_4@SiO_2$ modified with anti-mesothelin antibody; APTES, (3-aminopropyl)triethoxysilane; MRI, magnetic resonance imaging; TEOS, tetraethylorthosilicate; h, hours.

Figure 2 The electron microscopic image of A-MFS and its enlarged view (**A**), the distribution of hydrodynamic diameter (**B**), relaxation rate (r1, r2) of A-MFS versus Fe concentration (**C**), and XPS result (**D**).
Notes: A-MFS has a spherical appearance and a regular shape, and most of its hydrodynamic diameters range between 110 and 130 nm, r1 =0.549 mM/s and r2 =59.435 mM/s. A-MFS contains Fe, O, C, N, and Si.
Abbreviations: A-MFS, $Fe_3O_4@SiO_2$ modified with anti-mesothelin antibody; XPS, X-ray photoelectron spectroscopy.

The black central portion of the probe is the magnetic nucleus, with a larger electron density. The surrounding gray portion is the amorphous SiO_2 wrap. The size of the probe particle is uniform, and most of the hydrodynamic diameters range between 110 and 130 nm. The T2 relaxation rate of A-MFS is 59.435 mM/s and its T1 relaxation rate is 0.549 mM/s. Its relaxation rate is similar to others in the literature.[28] It means A-MFS can be used as negative contrast material. A-MFS has good stability of dispersion as shown in Figure S1. X-ray photoelectron spectroscopy detected that A-MFS contain Fe, O, C, N, and Si, so the result shows Si and antibodies are coated on the nanoparticle. Fe_3O_4 and SPIONs are most commonly used for preparation of multifunctional nanoparticles due to their unique superparamagnetic features, high stability, and biocompatibility. The superparamagnetic behavior of SPIONs is essential for MRI. Each SPION acts as a small magnet; therefore, SPIONs display increased magnetization and respond rapidly to external magnetic field. After removing the external magnetic field, magnetized nanoparticles are dissipated by a brief shaking. SPIONs shorten the tissue T2-weighted relaxation time to enhance tissue MRI contrast and, therefore, are widely used as T2 contrast agents. The high stability of SPIONs enables persistent circulation in the blood and accumulation in the target area. If the probe diameter exceeds 300 nm, they are phagocytosed by the reticuloendothelial system. They persist in the blood circulation and accumulate less in tissues. Silica is used as a surface modifier of nanoparticles due to its nontoxicity and stability. Fe_3O_4 is sealed by SiO_2 coating to improve its biocompatibility. The silica coating provides binding sites for the anti-MSLN antibody. Therefore, our team successfully synthesized the A-MFS probe with good magnetic properties and high stability.

Cytotoxicity of A-MFS
The cytotoxicity of FS modified with anti-MSLN antibody in SW1990 cells was determined using a CCK-8 assay. SW1990 cells were incubated with different concentrations (0, 100, 200, 300, 400, and 500 mg/L) of the target nanoprobe solutions. The CCK-8 assay showed that the A-MFS had dose-dependent cytotoxicity for SW1990 cells. As shown in Figure 3, with the increase in the concentration of A-MFS, the cell viability was above 86%, irrespective of the incubation period (2, 6, and 24 hours). The cell viability was higher than 95%, when the concentration of the probe was under 400 mg/L. In this study, the concentration of the probe was 1 mg/mL. Therefore, A-MFS was almost noncytotoxic, with potential biomedical applications. Fe is an essential element for human body; for example, it mediates the formation of hemoglobin and myohemoglobin and also associates with the activity of specific
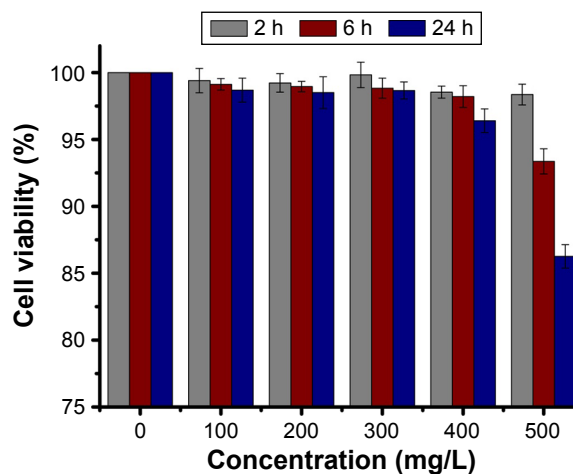
Figure 3 CCK-8 assay of SW1990 cell viability after incubation with different concentrations of A-MFS for 2, 6, and 24 hours.
Note: With the increase in the concentration of A-MFS from 0 to 500 mg/L, the cell viability exceeded 86%.
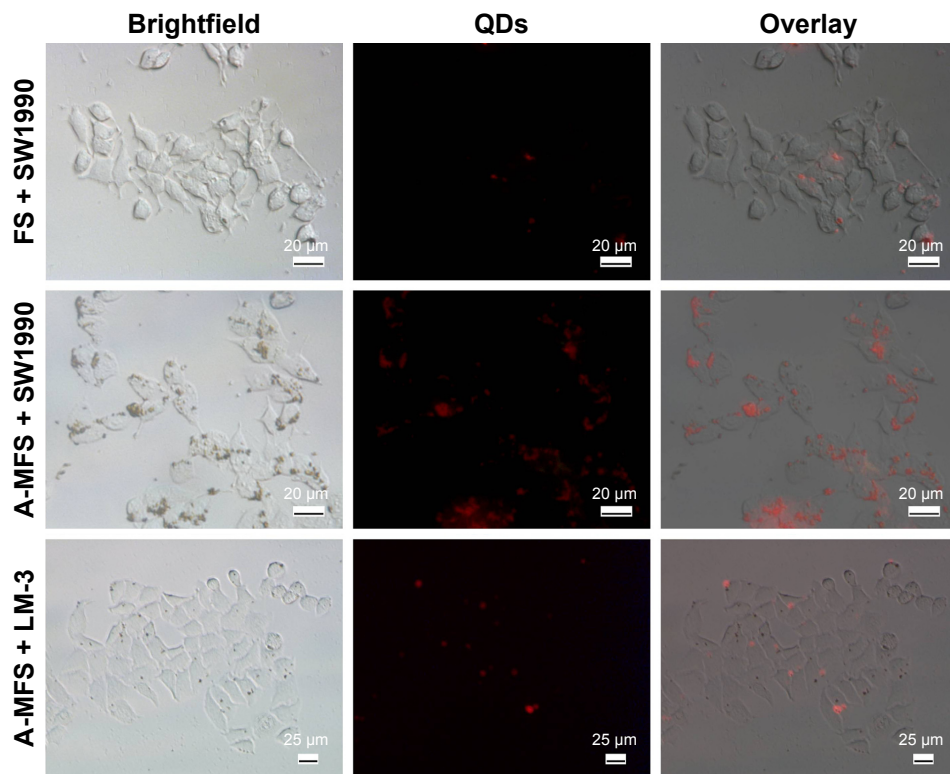**Abbreviations:** A-MFS, Fe_3O_4@SiO_2 modified with anti-mesothelin antibody; CCK-8, Cell Counting Kit-8.

enzymes in vivo. Therefore, SPIONs, including Fe_3O_4, are considered as safe contrast agents for imaging applications as they can be reduced to iron, which eventually contributes to the normal iron levels. The safety of silica is proven. In our study, A-MFS showed limited cytotoxicity and, therefore, is used in in vitro and in vivo studies.

In vitro targeting test
In vitro targeting test was performed by adding fluorescent quantum dots to nanoprobes to observe the cellular adsorption. Results shown in Figure 4 suggest that the red fluorescent dots were more frequently found on the surface of SW1990 cells, after incubation with A-MFS. The other two groups, SW1990 cells with FS and LM-3 cells with A-MFS, showed small red fluorescent dots on the surface of cells. Flow cytometric analysis showed that MSLN was expressed on the surface of SW1990 (Figure 5). The adsorption efficiency of the nanoprobe FS in SW1990 cells was increased significantly, after modification with anti-MSLN antibody. LM-3, the human liver cancer cell line, expressed little MSLN, while SW1990 cells expressed higher levels of MSLN as mentioned above. Results showed that the probe FS modified with anti-MSLN antibody recognized the SW1990 cells expressing MSLN. The findings demonstrate that FS modified with anti-MSLN antibody effectively targeted MSLN-expressing pancreatic cancer cells in vitro.

In vivo targeting by A-MFS
The in vivo MRI was successfully completed. The MRI T2-weighted images of nude mice are shown in Figure 6, and the quantitative tumor signal values are shown in Figure 7.

Figure 4 In vitro targeting test.
Note: The red fluorescent dots were found more frequently on the surface of SW1990 cells, after incubation with A-MFS.
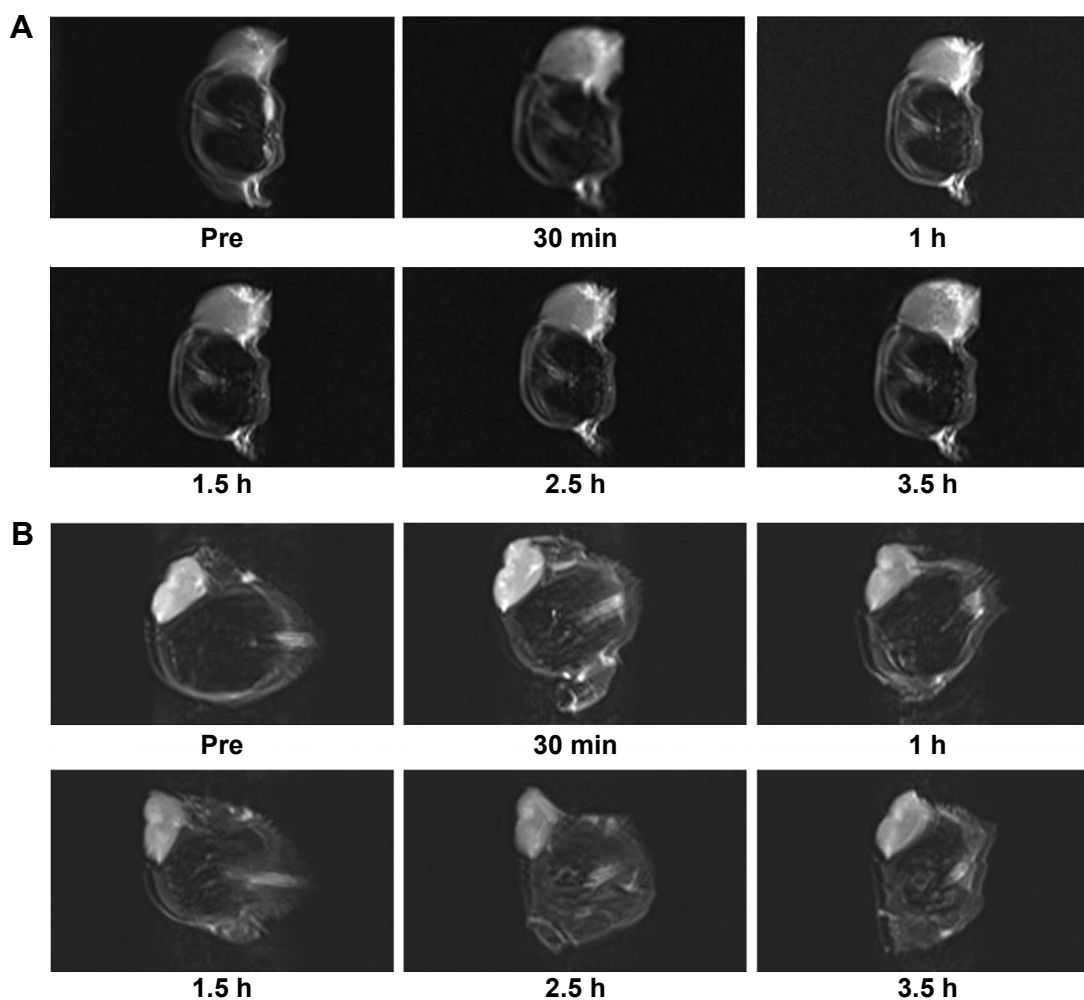**Abbreviations:** A-MFS, $Fe_3O_4@SiO_2$ modified with anti-mesothelin antibody; QD, quantum dot.
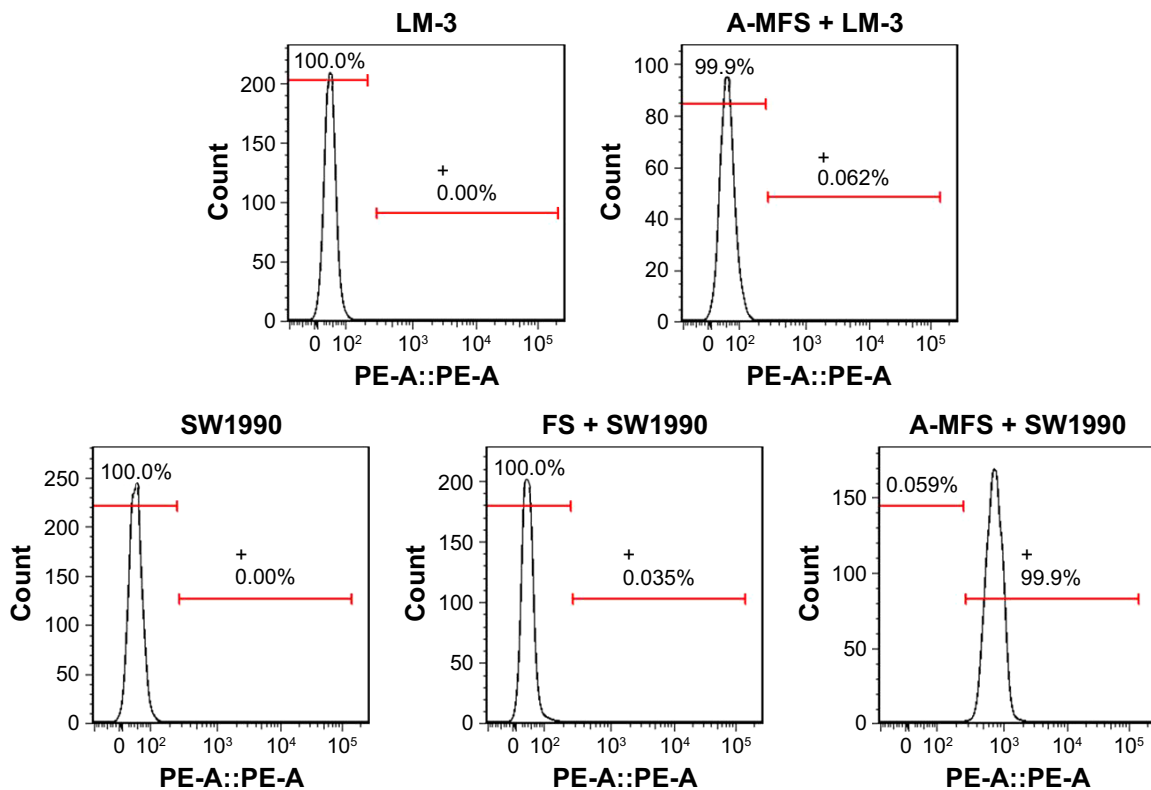

Figure 5 Flow cytometry.
Note: MSLN expressed on the surface of SW1990.
Abbreviations: A-MFS, $Fe_3O_4@SiO_2$ modified with anti-mesothelin antibody; FS, $Fe_3O_4@SiO_2$; MSLN, mesothelin; PE-A, Phycoerythrin-Conjugated Antibody.

Figure 6 (**A**) and (**B**) respectively represent T2-weighted images in MRI (3.0 T) of tumors in vivo before and after injection of saline solution and A-MFS.
Notes: The images were obtained at the following time points: before injection, 30 minutes later, 1, 1.5, 2.5, and 3.5 hours after injection. The tumor signal decreased after injection of A-MFS. When injected for 2.5 hours, the T2-weighted signal values decreased to the lowest level. The signal remained almost constant after injection of saline solution.
Abbreviations: A-MFS, $Fe_3O_4@SiO_2$ modified with anti-mesothelin antibody; MRI, magnetic resonance imaging; min, minutes; h, hours.
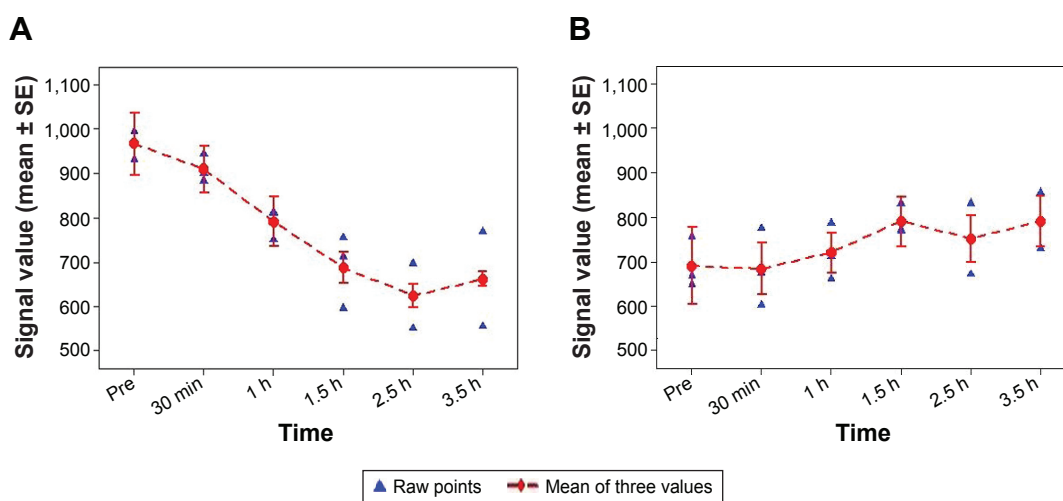
Figure 7 The T2-weighted quantitative signals of tumor before and after injection of A-MFS (**A**); the T2-weighted quantitative signal before and after injection of saline solution (**B**).
Notes: (**A**) Shows decreased tumor signal after injection of A-MFS via the mouse tail vein, and at ~2.5 hours, it decreased to the lowest level. (**B**) Illustrates the insignificant decrease in signal levels after injection of saline.
Abbreviations: A-MFS, $Fe_3O_4@SiO_2$ modified with anti-mesothelin antibody; SE, standard error.
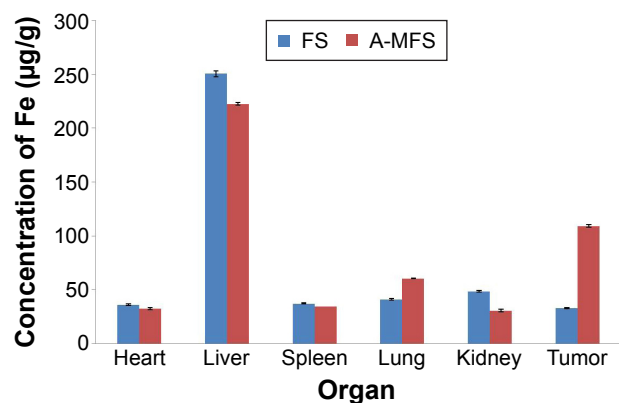
Figure 8 Fe distribution (µg/g) in heart, liver, spleen, lung, kidney, and tumor, before and after injection of FS and A-MFS intravenously via the tail vein.
Note: The Fe levels in the tumor differ significantly following injection of FS and A-MFS.
Abbreviations: A-MFS, $Fe_3O_4@SiO_2$ modified with anti-mesothelin antibody; FS, $Fe_3O_4@SiO_2$.

The T2 signal values of experimental group xenograft were decreased by 342.533±42.6 after injection of the target probe, and the control group was decreased by −61.233±33.9 after injection of saline solution, while the FS group decreased by −58.7±19.4 at 2.5 hours. The decrease of tumor signal by A-MFS was much more significant than that by saline and FS ($P<0.05$). Results could be seen in Figures S2 and S3. Similarly, the T2-weighted images showed that the tumor signal in the experimental group was decreased after injection of the probe FS modified with anti-MSLN antibody, while the control and FS groups were barely altered. Due to its paramagnetic properties, Fe_3O_4 acts as a negative contrast agent of MRI. It decreases the T2-weighted tissue signal to enhance the contrast by shortening the transverse relaxation time T2, suggesting that the nanoprobe selectively accumulated in the pancreatic cancer tissue, shortened the transverse relaxation time, and decreased signal of tissue. Therefore, FS modified with anti-MSLN antibody is a good T2 targeting agent in pancreatic cancer of nude mice. It may also be a promising and potential agent for clinical diagnosis of pancreatic cancer.

Fe distribution in organs

The distribution of Fe in vivo in mice injected with FS and A-MFS is illustrated in Figure 8. The Fe levels in the tumors of A-MFS group were obviously higher than in the FS group. The Fe levels in the lung were also increased. The Fe in other organs (heart, liver, spleen, and kidney) was approximately similar in A-MFS and FS groups. The xenografts of pancreatic cancer express higher MSLN levels than the other organs. MSLN is normally present on the mesothelial lining of the pleura. The visceral pleura cover the lung closely and directly and cannot be removed during the lung extraction. The results demonstrate that the probe FS modified with anti-MSLN antibody selectively accumulates in transplanted pancreatic cancer and pleural mesothelial cells. Both results showed that the probe targeted MSLN-expressing tissues and demonstrated effective in vivo targeting potential of A-MFS.

Pathology

Comparative histochemical analysis following hematoxylin and eosin staining of organs in the experimental (A-MFS) and control (saline solution) group mice is presented in Figure 9. The maps show no significant differences in histology between the two sets. Therefore, the targeting nanoparticle was completely nontoxic to mice and suggests potential for clinical application.
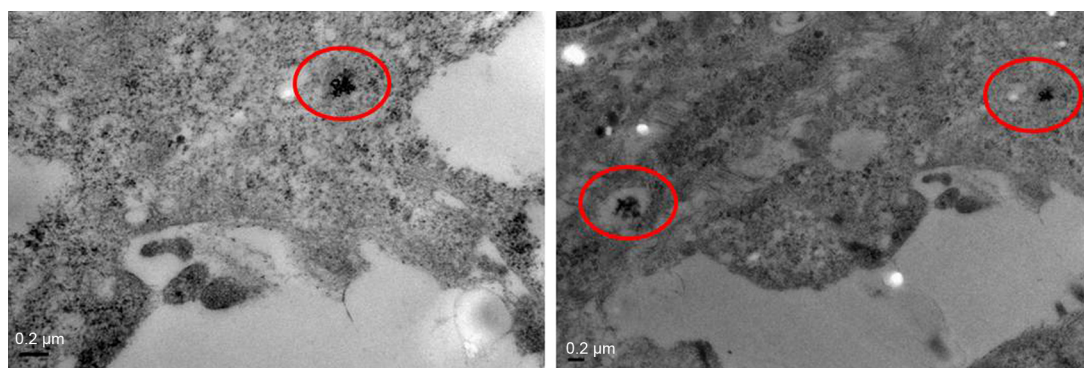
Transmission electron microscopy

As shown in Figure 10, the transmission electron microscopy of transplanted tumors treated with A-MFS revealed A-MFS accumulation in the tumor cells.
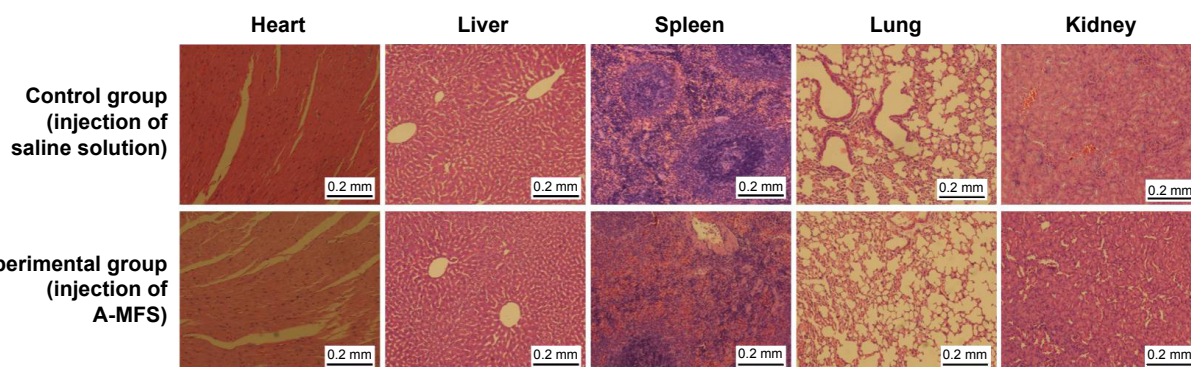
Figure 9 Histology of heart, liver, spleen, lung, and kidney in the two groups, following injection of saline solution and A-MFS, respectively.
Note: No obvious differences were seen in the control and experimental groups.
Abbreviation: A-MFS, $Fe_3O_4@SiO_2$ modified with anti-mesothelin antibody.

Figure 10 Transmission electron microscopy images.
Note: Black dots circled by red circles represent nanoparticles.

Conclusion

In this study, the FS probe was successfully prepared and coloaded with anti-MSLN antibody. Results showed stable and nontoxic A-MFS with regular morphology. Targeting a nanoprobe to the MSLN antigen is an effective contrast agent in pancreatic cancer cells. Our team demonstrated that A-MFS was capable of specifically recognizing the MSLN-expressing cells in vitro. In addition, A-MFS also exhibits excellent MRI properties and targeting potential to human pancreatic cancer xenografts in nude mice in vivo. Therefore, A-MFS effectively targets pancreatic cancer in vitro and in vivo. In conclusion, A-MFS represents a potential T2 contrast agent for the diagnosis of pancreatic cancer, and it will also be beneficial to find its metastasis.

Acknowledgments

Disclosure

The authors report no conflicts of interest in this work.

References

1. Tannery KM, Rizzolo D. Pancreatic cancer: practical strategies for early diagnosis and management. *JAAPA*. 2013;26(10):27–32.
2. Wolfgang CL, Herman JM, Laheru DA, et al. Recent progress in pancreatic cancer. *CA Cancer J Clin*. 2013;63(5):318–348.
3. Chang MC, Wong JM, Chang YT. Screening and early detection of pancreatic cancer in high risk population. *World J Gastroenterol*. 2014; 20(9):2358–2364.
4. Muniraj T, Jamidar PA, Aslanian HR. Pancreatic cancer: a comprehensive review and update. *Dis Mon*. 2013;59(11):368–402.
5. Kaur S, Baine MJ, Jain M, Sasson AR, Batra SK. Early diagnosis of pancreatic cancer: challenges and new developments. *Biomark Med*. 2012; 6(5):597–612.
6. Chen ZY, Wang YX, Lin Y, et al. Advance of molecular imaging technology and targeted imaging agent in imaging and therapy. *Biomed Res Int*. 2014;2014:819324.
7. Weissleder R, Pittet MJ. Imaging in the era of molecular oncology. *Nature*. 2008;452(7187):580–589.
8. Mankoff DA, Pryma DA, Clark AS. Molecular imaging biomarkers for oncology clinical trials. *J Nucl Med*. 2014;55(4):525–528.
9. Chan A, Prassas I, Dimitromanolakis A, et al. Validation of biomarkers that complement CA19.9 in detecting early pancreatic cancer. *Clin Cancer Res*. 2014;20(22):5787–5795.
10. Hanada K, Okazaki A, Hirano N, et al. Diagnostic strategies for early pancreatic cancer. *J Gastroenterol*. 2015;50(2):147–154.
11. Hollingsworth MA, Swanson BJ. Mucins in cancer: protection and control of the cell surface. *Nat Rev Cancer*. 2004;4(1):45–60.
12. Qu CF, Li Y, Song YJ, et al. MUC1 expression in primary and metastatic pancreatic cancer cells for in vitro treatment by (213)Bi-C595 radioimmunoconjugate. *Br J Cancer*. 2004;91(12):2086–2093.
13. Andrianifahanana M, Moniaux N, Schmied BM, et al. Mucin (MUC) gene expression in human pancreatic adenocarcinoma and chronic pancreatitis: a potential role of MUC4 as a tumor marker of diagnostic significance. *Clin Cancer Res*. 2001;7(12):4033–4040.
14. Park JY, Hiroshima Y, Lee JY, Maawy AA, Hoffman RM, Bouvet M. MUC1 selectively targets human pancreatic cancer in orthotopic nude mouse models. *PLoS One*. 2015;10(3):e0122100.
15. Wu SC, Chen YJ, Lin YJ, Wu TH, Wang YM. Development of a mucin4-targeting SPIO contrast agent for effective detection of pancreatic tumor cells in vitro and in vivo. *J Med Chem*. 2013;56(22): 9100–9109.
16. Ren YQ, Zhang HY, Su T, Wang XH, Zhang L. Clinical significance of serum survivin in patients with pancreatic ductal adenocarcinoma. *Eur Rev Med Pharmacol Sci*. 2014;18(20):3063–3068.
17. Bobustuc GC, Patel A, Thompson M, et al. MGMT inhibition suppresses survivin expression in pancreatic cancer. *Pancreas*. 2015;44(4): 626–635.
18. Tong M, Xiong F, Shi Y, et al. In vitro study of SPIO-labeled human pancreatic cancer cell line BxPC-3. *Contrast Media Mol Imaging*. 2013; 8(2):101–107.
19. Xue A, Xue M, Jackson C, Smith RC. Suppression of urokinase plasminogen activator receptor inhibits proliferation and migration of pancreatic adenocarcinoma cells via regulation of ERK/p38 signaling. *Int J Biochem Cell Biol*. 2009;41(8–9):1731–1738.
20. Gorantla B, Asuthkar S, Rao JS, Patel J, Gondi CS. Suppression of the uPAR-uPA system retards angiogenesis, invasion, and in vivo tumor development in pancreatic cancer cells. *Mol Cancer Res*. 2011;9(4): 377–389.
21. Yang L, Mao H, Cao Z, et al. Molecular imaging of pancreatic cancer in an animal model using targeted multifunctional nanoparticles. *Gastroenterology*. 2009;136(5):1514–1525.e1512.

22. Brackett D, Postier R, Raffeld M, Lerner M, Laszik ZG, Hassan R. Mesothelin is overexpressed in pancreaticobiliary adenocarcinomas but not in normal pancreas and chronic pancreatitis. *Am J Clin Pathol*. 2005;124(6):838–845.

23. Argani P, Iacobuzio-Donahue C, Ryu B, et al. Mesothelin is overexpressed in the vast majority of ductal adenocarcinomas of the pancreas: identification of a new pancreatic cancer marker by serial analysis of gene expression (SAGE). *Clin Cancer Res*. 2001;7(12):3862–3868.

24. Chen SH, Hung WC, Wang P, Paul C, Konstantopoulos K. Mesothelin binding to CA125/MUC16 promotes pancreatic cancer cell motility and invasion via MMP-7 activation. *Sci Rep*. 2013;3:1870.

25. Tang Z, Qian M, Ho M. The role of mesothelin in tumor progression and targeted therapy. *Anticancer Agents Med Chem*. 2013;13(2): 276–280.

26. Yamasaki S, Miura Y, Davydova J, Vickers SM, Yamamoto M. Intravenous genetic mesothelin vaccine based on human adenovirus 40 inhibits growth and metastasis of pancreatic cancer. *Int J Cancer*. 2013;133(1): 88–97.

27. Zheng C, Jia W, Tang Y, Zhao H, Jiang Y, Sun S. Mesothelin regulates growth and apoptosis in pancreatic cancer cells through p53-dependent and -independent signal pathway. *J Exp Clin Cancer Res*. 2012;31:84.

28. Deng L, Ke X, He Z, et al. A MSLN-targeted multifunctional nanoimmunoliposome for MRI and targeting therapy in pancreatic cancer. *Int J Nanomedicine*. 2012;7:5053–5065.

29. Dong A, Lan S, Huang J, et al. Modifying Fe_3O_4-functionalized nanoparticles with N-halamine and their magnetic/antibacterial properties. *ACS Appl Mater Interfaces*. 2011;3(11):4228–4235.

30. Wahajuddin AS. Superparamagnetic iron oxide nanoparticles: magnetic nanoplatforms as drug carriers. *Int J Nanomedicine*. 2012; 7:3445–3471.

31. Singh AK, Hahn MA, Gutwein LG, et al. Multi-dye theranostic nanoparticle platform for bioimaging and cancer therapy. *Int J Nanomedicine*. 2012;7:2739–2750.

32. Ding HL, Zhang YX, Wang S, Xu JM, Xu SC, Li GH. $Fe_3O_4@SiO_2$ core/shell nanoparticles: the silica coating regulations with a single core for different core sizes and shell thicknesses. *Chem Mater*. 2012;24(23): 4572–4580.

33. Uribe Madrid SI, Pal U, Kang YS, Kim J, Kwon H, Kim J. Fabrication of $Fe_3O_4@mSiO_2$ core-shell composite nanoparticles for drug delivery applications. *Nanoscale Res Lett*. 2015;10:217.

34. Tang Y, Liang S, Yu S, et al. Enhanced adsorption of humic acid on amine functionalized magnetic mesoporous composite microspheres. *Colloids Surf A Physicochem Eng Asp*. 2012;406:61–67.

35. Xing H, Bu W, Zhang S, et al. Multifunctional nanoprobes for upconversion fluorescence, MR and CT trimodal imaging. *Biomaterials*. 2012; 33(4):1079–1089.

Supplementary materials
Stability of dispersion test

In order to observe the stability of A-MFS in solution, different concentrations of A-MFS solutions (50 mg/mL, 100 µg/mL, 150 µg/mL, 200 µg/mL) were rested at room temperature for different times (0, 4, 24 hours). The optical images were taken to reflect their stability. Results show that the nanoparticle has a good dispersion at macro level, as shown in Figure S1.

In vivo MRI test of FS

Three mice were injected with 1 mg/mL of $Fe_3O_4@SiO_2$ (FS) (0.1 mL per mouse), respectively, via caudal veins. All the images of mice were obtained using Siemens 3.0 T magnetic resonance scanner. The T2 signal values of xenograft were decreased by -58.7 ± 19.4 after injection of the FS at 2.5 hours. Results showed that the decrease of tumor signal by A-MFS was much more significant than that by FS ($P<0.05$). Images are shown in Figures S1 and S2. It should be noted that the decrease of tumor signal by FS at 5 hours (53.7 ± 15.1) was also more significant than that by saline ($P<0.05$). It may be the result of passive targeting of material. But, the decrease of signal by FS at 5 hours is still less than that by A-MFS.

0 hour   **4 hours**   **24 hours**
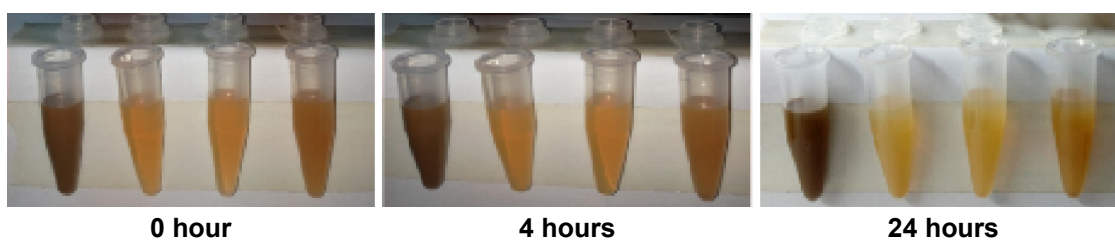
Figure S1 Stability of A-MFS solution with different concentrations.
Abbreviation: A-MFS, anti-mesothelin antibody.

Pre   **30 minutes**   **1 hour**

1.5 hours   **2.5 hours**   **3.5 hours**
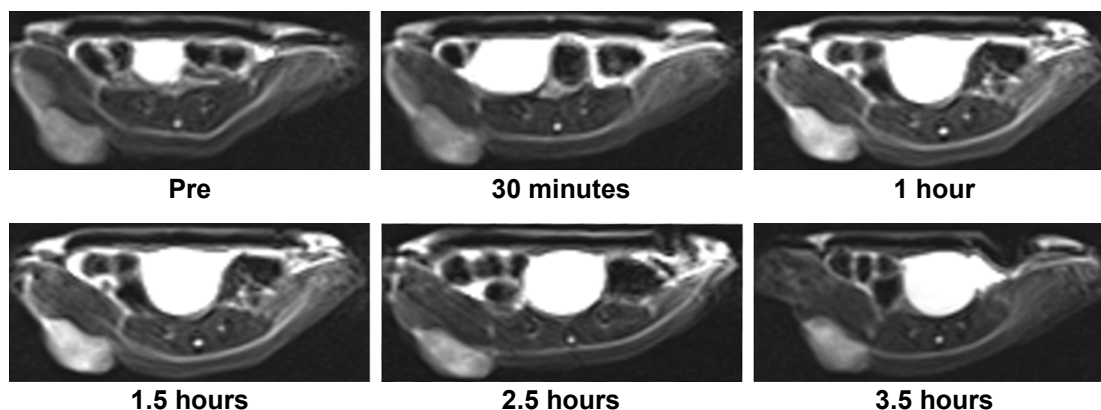
Figure S2 MRI T2 images of FS group.
Note: The signal of xenograft did not decrease significantly after injection of FS.
Abbreviations: MRI, magnetic resonance imaging; FS, $Fe_3O_4@SiO_2$.
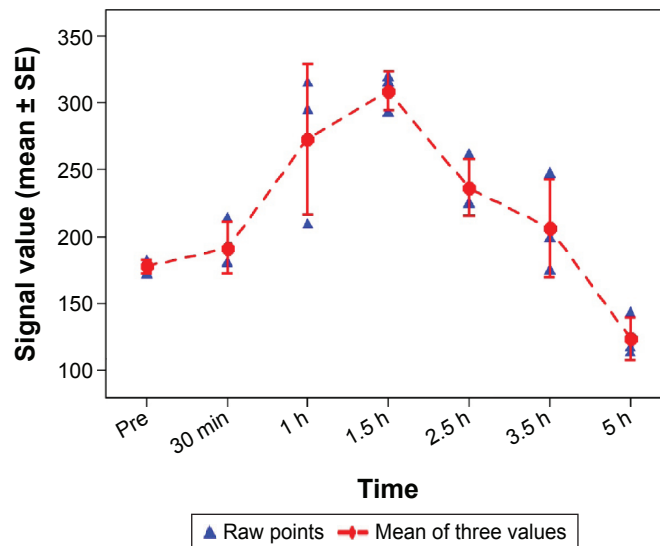
Figure S3 The T2-weighted quantitative signals of tumor before and after injection of FS.
Note: The signal of xenograft did not decrease significantly after injection of FS.
Abbreviations: FS, $Fe_3O_4@SiO_2$; SE, standard error; min, minutes; h, hours.